RAA 2020 Vol. **20** No. **1**, 10(6pp) doi: 10.1088/1674–4527/20/1/10

http://www.raa-journal.org *http://iopscience.iop.org/raa*

Research in Astronomy and Astrophysics

Photometric investigation on the W-subtype contact binary V1197 Her

Xiao Zhou[1,2,3,4] and Boonrucksar Soonthornthum[2]

[1] Yunnan Observatories, Chinese Academy of Sciences, Kunming 650216, China; *zhouxiaophy@ynao.ac.cn*
[2] National Astronomical Research Institute of Thailand, 260 Moo 4, T. Donkaew, A. Maerim, Chiangmai, 50180, Thailand
[3] Key Laboratory of the Structure and Evolution of Celestial Objects, Chinese Academy of Sciences, Kunming 650216, China
[4] Center for Astronomical Mega-Science, Chinese Academy of Sciences, Beijing 100101, China

Received 2019 May 30; accepted 2019 August 2

Abstract Multi-color light curves of V1197 Her were obtained with the 2.4 meter optical telescope at the Thai National Observatory and the Wilson-Devinney (W-D) program was used to model the observational light curves. The photometric solutions reveal that V1197 Her is a W-subtype shallow contact binary system with a mass ratio of $q = 2.61$ and a fill-out factor of $f = 15.7\%$. The temperature difference between the primary star and secondary star is only 140 K in spite of the low degree of contact, which means that V1197 Her is not only in geometrical contact configuration but is also already under thermal contact status. The orbital inclination of V1197 Her is as high as $i = 82.7°$, and the primary star is completely eclipsed at the primary minimum. The totally eclipsing characteristic implies that the determined physical parameters are highly reliable. The masses, radii and luminosities of the primary star (star 1) and secondary star (star 2) are estimated to be $M_1 = 0.30(1)\,M_\odot$, $M_2 = 0.77(2)\,M_\odot$, $R_1 = 0.54(1)\,R_\odot$, $R_2 = 0.83(1)\,R_\odot$, $L_1 = 0.18(1)\,L_\odot$ and $L_2 = 0.38(1)\,L_\odot$. The evolutionary statuses of the two component stars are drawn in the Hertzsprung-Russell diagram, showing that the less massive but hotter primary star is more evolved than the secondary star. The period of V1197 Her is decreasing continuously at a rate of $dP/dt = -2.58 \times 10^{-7}$ day · year^{-1}, which can be explained by mass transfer from the more massive star to the less massive one at a rate of $\frac{dM_2}{dt} = -1.61 \times 10^{-7}\,M_\odot$ year^{-1}. The light curves of V1197 Her are reported to show the O'Connell effect. Thus, a cool spot is added to the more massive star to model the asymmetry in the light curves.

Key words: techniques: photometric — binaries: eclipsing — stars: fundamental parameters

1 INTRODUCTION

Contact binaries, also known as W UMa type binaries, are typical interaction binaries in the Universe. The evolutionary scenarios of contact binaries are quite different from those of single stars due to the existence of a common envelope surrounding the component stars in contact binary systems. Over the past few decades, photometric and spectrometric data on contact binaries have been accumulating rapidly owing to the large sky survey projects such as the Optical Gravitational Lensing Experiment (OGLE) (Udalski et al. 1992), the All Sky Automated Survey (ASAS) (Pojmanski 1997), the Wide Angle Search for Planets (SuperWASP) (Street et al. 2003), the Large Sky Area Multi-Object Fibre Spectroscopic Telescope (LAMOST) (Zhao et al. 2012; Qian et al. 2017, 2019) and the Gaia mission (Gaia Collaboration et al. 2016, 2018). Contact binaries are useful tools for studying a wide range of astrophysical problems (e.g., testing stellar evolution models, and searching for peculiar stars) and are becoming more and more important.

V1197 Her is an EW type eclipsing binary with a period of $P = 0.262680$ days as listed in the International Variable Star Index (VSX) (Watson et al. 2006). The target has been neglected since it was discovered. Neither radial velocity nor light curve has been presented before. Only the surface effective temperature has been derived by the Gaia mission, published in Gaia Data Release 2 as $T = 4973$ K. In the present work, we study contact binary V1197 Her thoroughly for the first time. Observations of complete light curves and mid-eclipse times are illustrated in Section 2. Analyses on its period variations are presented in Section 3. Modeling of light curves is in

Table 1 Coordinates and V Band Magnitudes

Target	α_{2000}	δ_{2000}	$V_{\rm mag}$
V1197 Her	$16^{\rm h}33^{\rm m}22.855^{\rm s}$	$+28°18'19.475''$	13.378
UCAC4 592–055825	$16^{\rm h}33^{\rm m}20.995^{\rm s}$	$+28°16'16.089''$	13.678
UCAC4 592–055831	$16^{\rm h}33^{\rm m}24.531^{\rm s}$	$+28°15'54.818''$	14.637

Section 4. Discussion and conclusions are presented in the last section.

2 OBSERVATIONS AND DATA REDUCTION

The complete light curves of V1197 Her were obtained on 2016 April 20, 2016 April 25 and 2019 April 9 with the 2.4 meter optical telescope at the Thai National Observatory (TNO 2.4 m), National Astronomical Research Institute of Thailand (NARIT). The field of view (FOV) is 16×16 square arc-minutes and the terminal is equipped with a 4K×4K CCD camera (Soonthornthum 2018). Johnson-Cousins' BVR_CI_C filters were used during the observations. All observational images were reduced with the Image Reduction and Analysis Facility (IRAF) (Tody 1986). UCAC4 592-055825 and UCAC4 592-055831 in the same FOV were selected as the Comparison star (C) and Check star (Ch) as a differential photometry method was adopted to determine the light variations of V1197 Her. Their coordinates in the J2000.0 epoch and V band magnitudes are listed in Table 1. The observational light curves are displayed in Figure 1. Heliocentric Julian Dates (HJDs) are converted to phases with the following equation:

$$\mathrm{Min.I(HJD)} = 2458583.2589 + 0^{\rm d}.262680 \times E. \quad (1)$$

The initial epoch used in Equation (1) was obtained on 2019 April 9 and parabola fit on the observed light minimum was performed. In all, we got two mid-eclipse times with the TNO 2.4 m, which are listed in Table 2.

V1197 Her was also monitored by the 1 meter telescope (YNOs 1 m) and the 60 centimeter telescope (YNOs 60 cm) at the Yunnan Observatories, Chinese Academy of Sciences. A total of two primary (p) minima and four secondary (s) minima were determined by YNOs 1 m and YNOs 60 cm. The mid-eclipse times are also listed in Table 2.

3 INVESTIGATION OF THE PERIOD VARIATION

The period of a close binary is not always constant, especially for a semi-detached binary and contact binary due to possible mass transfer between component stars. Thus, the $O-C$ method is used to analyze the period variations of V1197 Her. All available mid-eclipse times are listed Table 3.

Column 1 - HJD of the observed mid-eclipse times (HJD - 2400000);

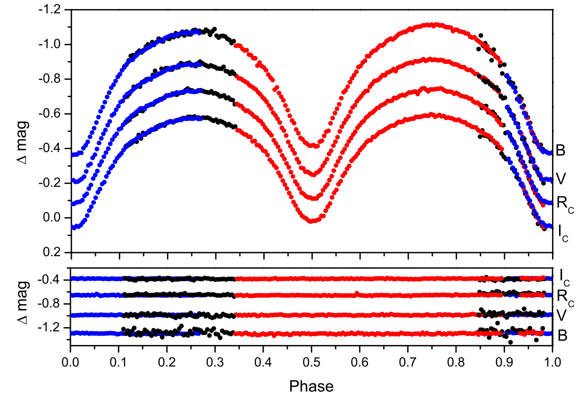

Fig. 1 The *black*, *red* and *blue colors* refer to data obtained on 2016 April 20, 2016 April 25 and 2019 April 9, respectively. The BVR_CI_C band light curves of V1197 Her are shown in the top panel and magnitude differences between the Comparison star and the Check star are displayed in the bottom panel.

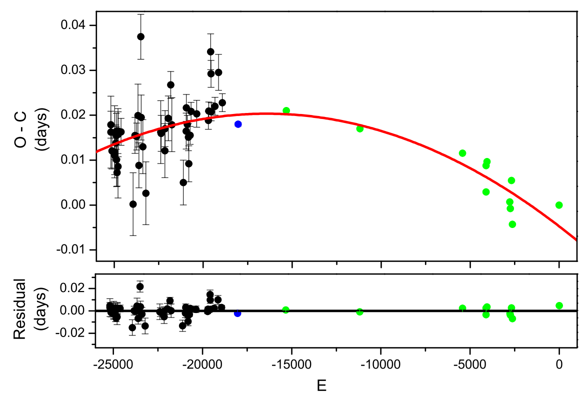

Fig. 2 The *black*, *blue* and *green colors* refer to mid-eclipse times obtained by visual, photoelectric and Charge Coupled Device observations, respectively. The *red line* represents the theoretical $O-C$ curve based on Equation (2).

Column 2 - primary (p) or secondary (s) mid-eclipse times;

Column 3 - calculated cycle numbers from the initial epoch;

Column 4 - the $O-C$ values calculated from Equation (1);

Column 5 - observational errors of mid-eclipse times;

Column 6 - vis, pe and CCD refer to visual, photoelectric and Charge Coupled Device observations;

Column 7 - references.

As displayed in Figure 2, the period of V1197 Her is not constant. Therefore, parabola fit is performed on the data and a new ephemeris is determined:

$$\begin{aligned}\mathrm{Min.I} =& 2458583.25417(\pm0.00006)\\ &+ 0.26267695(\pm0.00000001) \times E \\ &- 9.28(\pm0.06) \times 10^{-11} \times E^2 .\end{aligned} \quad (2)$$

Table 2 New CCD Times of Mid-eclipse Times

JD (Hel.)	Error (days)	p/s	Filter	Date	Telescope
2457504.3096	±0.0001	s	$B\ V\ R_C\ I_C$	2016 April 25	TNO 2.4 m
2457505.2231	±0.0003	p	$R_C\ I_C$	2016 April 26	YNOs 60 cm
2457517.1818	±0.0002	s	R_C	2016 May 8	YNOs 60 cm
2457855.3733	±0.0002	p	$V\ R_C$	2017 April 11	YNOs 60 cm
2457863.3836	±0.0002	s	$V\ R_C$	2017 April 19	YNOs 60 cm
2457878.3626	±0.0001	s	$V\ R_C\ I_C$	2016 May 4	YNOs 1 m
2457893.3256	±0.0002	s	$B\ V\ R_C\ I_C$	2016 May 19	YNOs 60 cm
2458583.2589	±0.0001	p	$B\ V\ R_C\ I_C$	2019 April 9	TNO 2.4 m

The newly determined ephemeris reveals that the period of V1197 Her is decreasing continuously at a rate of $dP/dt = -2.58 \times 10^{-7}\,\mathrm{day \cdot year^{-1}}$.

4 MODELING THE LIGHT CURVES

V1197 Her is a newly reported eclipsing binary. Analyses of its light curves have been neglected and this is the first time that complete multi-color light curves have been obtained. To find the physical parameters of V1197 Her, the Wilson-Devinney (W-D) program (Wilson, & Devinney 1971; Wilson 2012) is applied to model the light curves displayed in Figure 1. V1197 Her shows EW type light curves. Thereforce, Mode 3 for overcontact binaries is selected. The mean surface temperature of the secondary star (star 2) is fixed as $T_2 = 4973\,\mathrm{K}$ based on Gaia Data Release 2 (Gaia DR2) (Gaia Collaboration et al. 2016, 2018), and the star eclipsed at primary minimum is assumed to be the primary star. The free parameters include mass ratio ($q = M_2/M_1$), orbital inclination (i), modified dimensionless surface potential of star 1 (Ω_1), mean surface temperature of star 1 (T_1), and bandpass luminosities of star 1 (L_1). As the light curve is asymmetric, the latitude, longitude, angular radius and dimensionless temperature factor for a spot are also adjustable. At first, we run the W-D program with a fixed q value (q-search method) to find the proper mass ratio for the binary system. The results suggest that the best fit mass ratio is $q = 2.60$ as displayed in Figure 3. Then, we set the mass ratio as a free parameter together with other parameters and give the initial value as $q = 2.60$ to find a convergent solution. The final solutions for all elements are listed in Table 4 and the theoretical light curves are plotted in Figure 4. The geometrical structure of V1197 Her at Phase 0, 0.25, 0.50 and 0.75 are shown in Figure 5. The location of the spot we added in star 2 can be easily seen in Figure 5. Also, we have tried to set third light (l_3) as a free parameter when running the W-D program since tertiary components are commonly reported in contact binaries (Yang et al. 2016; Li et al. 2019). However, no convergent solution is acquired in that case.

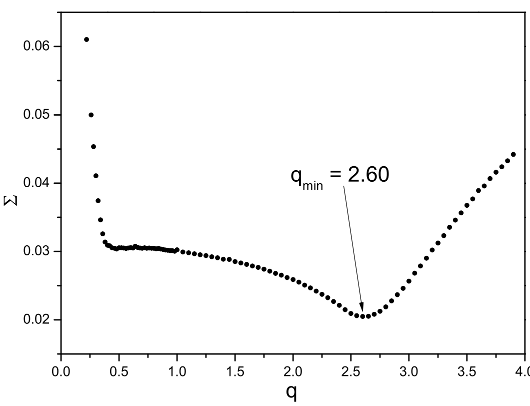

Fig. 3 The q-search diagram.

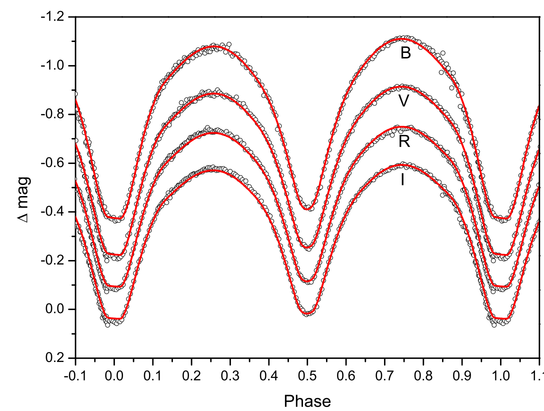

Fig. 4 The *open circles* are observational light curves obtained using the TNO 2.4 m. The *red lines* are theoretical light curves calculated with the Wilson-Devinney program.

5 DISCUSSION AND CONCLUSIONS

The photometric solutions for V1197 Her are determined for the first time based on the multi-color light curves obtained with the TNO 2.4 m telescope. According to the results listed in Table 4, V1197 Her is a W-subtype shallow contact binary with a mass ratio of $q = 2.61(4)$ and a fill-out factor of $f = 15.7(9.2)\%$. The primary star (star 1) is $140(5)\,\mathrm{K}$ hotter than the more massive secondary star (star 2). V1197 Her has a very high orbital inclination ($i = 82.7°$) and the geometrical structure at Phase $= 0$ (Fig. 5) shows that the primary star is totally eclipsed by the secondary star, which means that V1197 Her is a completely eclipsing binary system and the determined parameters in Table 4 are very reliable (Terrell & Wilson 2005; Li et al. 2018; He et al. 2019). Based on the mean surface tem-

Table 3 Mid-eclipse Times and $O-C$ Values for V752 Cen

JD(Hel.) (2400000+) (1)	p/s (2)	Epoch (3)	$O-C$ (days) (4)	Error (days) (5)	Method (6)	Ref. (7)
51967.548	s	–25185.5	0.0162	0.008	vis	[1]
51967.681	p	–25185	0.0179	0.003	vis	[1]
51984.618	s	–25120.5	0.0120	0.004	vis	[1]
52022.448	s	–24976.5	0.0161	0.006	vis	[1]
52022.575	p	–24976	0.0118	0.005	vis	[1]
52023.625	p	–24972	0.0111	0.005	vis	[1]
52041.490	p	–24904	0.0138	0.004	vis	[1]
52048.584	p	–24877	0.0155	0.002	vis	[1]
52049.373	p	–24874	0.0164	0.004	vis	[1]
52049.498	s	–24873.5	0.0101	0.006	vis	[1]
52059.477	s	–24835.5	0.0072	0.003	vis	[1]
52072.481	p	–24786	0.0086	0.007	vis	[1]
52074.459	s	–24778.5	0.0165	0.005	vis	[1]
52075.509	s	–24774.5	0.0158	0.005	vis	[1]
52117.407	p	–24615	0.0163	0.003	vis	[1]
52296.670	s	–23932.5	0.0002	0.007	vis	[1]
52323.610	p	–23830	0.0155	0.004	vis	[1]
52347.645	s	–23738.5	0.0153	0.003	vis	[1]
52367.482	p	–23663	0.0199	0.007	vis	[1]
52382.575	s	–23605.5	0.0088	0.005	vis	[1]
52409.397	s	–23503.5	0.0375	0.005	vis	[1]
52415.552	p	–23480	0.0195	0.005	vis	[1]
52438.530	s	–23392.5	0.0130	0.006	vis	[1]
52485.408	p	–23214	0.0026	0.007	vis	[1]
52702.658	p	–22387	0.0163	0.007	vis	[2]
52708.568	s	–22364.5	0.0160	0.004	vis	[2]
52764.515	s	–22151.5	0.0121	0.006	vis	[2]
52766.490	p	–22144	0.0170	0.004	vis	[2]
52813.512	p	–21965	0.0193	0.005	vis	[2]
52850.426	s	–21824.5	0.0268	0.003	vis	[3]
52867.360	p	–21760	0.0179	0.006	vis	[3]
53035.725	p	–21119	0.0050	0.005	vis	[3]
53079.604	p	–20952	0.0165	0.004	vis	[3]
53082.630	s	–20940.5	0.0216	0.003	vis	[3]
53095.629	p	–20891	0.0180	0.002	vis	[3]
53112.569	s	–20826.5	0.0151	0.003	vis	[3]
53117.554	s	–20807.5	0.0092	0.004	vis	[3]
53137.524	s	–20731.5	0.0155	0.002	vis	[3]
53150.532	p	–20682	0.0209	0.002	vis	[3]
53233.407	s	–20366.5	0.0203	0.003	vis	[4]
53406.643	p	–19707	0.0189	0.002	vis	[4]
53411.636	p	–19688	0.0209	0.002	vis	[4]
53440.544	p	–19578	0.0341	0.004	vis	[4]
53445.530	p	–19559	0.0292	0.003	vis	[4]
53447.623	p	–19551	0.0208	0.002	vis	[4]
53502.393	s	–19342.5	0.0220	0.002	vis	[4]
53557.432	p	–19133	0.0295	0.004	vis	[4]
53611.406	s	–18927.5	0.0228	0.002	vis	[4]
53846.4998	s	–18032.5	0.0180	0.0004	pe	[5]
54556.9209	p	–15328	0.0210	0.0001	CCD	[6]
55643.8867	p	–11190	0.0170	0.0001	CCD	[7]
57156.7867	s	–5430.5	0.0115	0.0002	CCD	[8]
57504.3096	s	–4107.5	0.0088	0.0001	CCD	[9]
57505.2231	p	–4104	0.0029	0.0003	CCD	[9]
57517.1818	s	–4058.5	0.0097	0.0002	CCD	[9]
57855.3733	p	–2771	0.0007	0.0002	CCD	[9]
57863.3836	s	–2740.5	–0.0008	0.0002	CCD	[9]
57878.3626	s	–2683.5	0.0055	0.0001	CCD	[9]
57893.3256	s	–2626.5	–0.0043	0.0002	CCD	[9]
58583.2589	p	0	0	0.0001	CCD	[9]

[1] BBSAG Bulletins (`https://www.astronomie.info/bbsag/bulletins.html`); [2] Diethelm (2003); [3] Diethelm (2004); [4] Locher (2005); [5] Diethelm (2006); [6] Nelson (2009); [7] Nelson (2012); [8] Nelson (2016); [9] The present work.

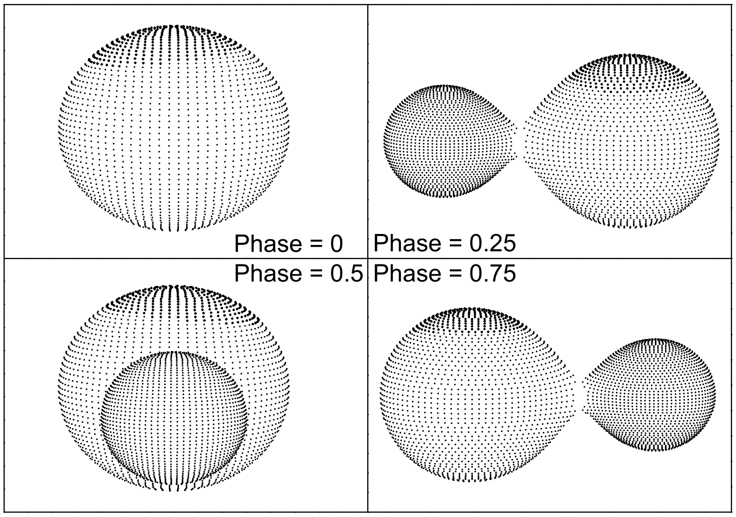

Fig. 5 The geometrical structure at Phase = 0, Phase = 0.25, Phase = 0.5 and Phase = 0.75.

perature of star 2 ($T_2 = 4973\,$K), its mass is estimated to be $M_2 = 0.77(2)\,M_\odot$ (Cox 2000). Then, the masses, radii and luminosities of the two component stars in V1197 Her are calculated, and are listed in Table 5. The orbital semi-major axis of this binary system is calculated to be $a = 1.76(2)\,R_\odot$. The evolutionary status of the primary star and secondary star are plotted in the Hertzsprung-Russell (H-R) diagram (Fig. 6), which implies that the secondary star is still a main sequence star while the primary star has evolved away from the main sequence stage. The period variations of V1197 Her are revealed to be decreasing continuously at a rate of $dP/dt = -2.58 \times 10^{-7}\,\mathrm{day \cdot year^{-1}}$, which may be due to the mass transfer from the more massive star (star 2) to the less massive one (star 1) (He et al. 2016; Liao et al. 2019). The mass transfer rate is estimated to be $\frac{dM_2}{dt} = -1.61 \times 10^{-7}\,M_\odot\,\mathrm{year}^{-1}$.

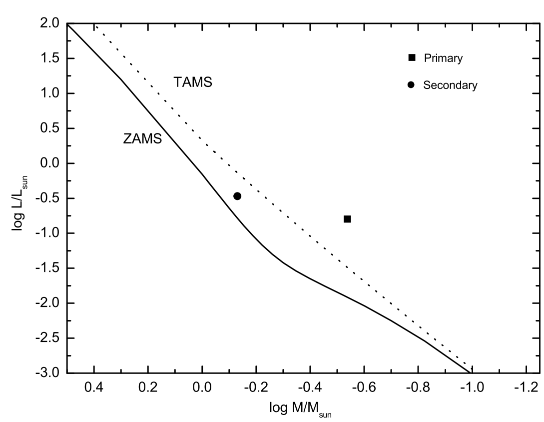

Fig. 6 The H - R diagram.

The negative O'Connell effect is observed to appear on the light curves of V1197 Her, in which the light maximum at phase 0.75 (Max II) is brighter than the light maximum at phase 0.25 (Max I). The magnitude difference between the two light maxima (Max I - Max II) is 0.031 mag in B band, 0.027 mag in V band, 0.022 mag in R_c band and 0.019 mag in I_c band. It is suggested that magnetic activity of the component stars mainly account for the O'Connell effect in solar-type or late-type contact binaries (Qian et al. 2014; Xiao et al. 2016; Li et al. 2017). Some interesting

Table 4 Photometric Solutions for V1197 Her

Parameters	Values
T_1 (K)	5113($\pm$5)
q (M_2/M_1)	2.61($\pm$0.04)
$i(^\circ)$	82.7($\pm$0.3)
T_2 (K)	4973(fixed)
ΔT (K)	140($\pm$5)
T_2/T_1	0.973($\pm$0.001)
$L_1/(L_1+L_2)\,(B)$	0.3408($\pm$0.0008)
$L_1/(L_1+L_2)\,(V)$	0.3316($\pm$0.0008)
$L_1/(L_1+L_2)\,(R_c)$	0.3247($\pm$0.0012)
$L_1/(L_1+L_2)\,(I_c)$	0.3203($\pm$0.0014)
r_1 (pole)	0.287($\pm$0.001)
r_1 (side)	0.300($\pm$0.002)
r_1 (back)	0.338($\pm$0.002)
r_2 (pole)	0.443($\pm$0.005)
r_2 (side)	0.475($\pm$0.007)
r_2 (back)	0.504($\pm$0.010)
$\Omega_1 = \Omega_2$	6.00($\pm$0.06)
f	15.7 %($\pm$9.2 %)
$\theta(^\circ)$	6.5($\pm$1.4)
$\psi(^\circ)$	106.2($\pm$3.0)
r(rad)	0.75($\pm$0.07)
T_f	0.82($\pm$0.07)
$\Sigma\omega(O-C)^2$	0.0179

Table 5 Absolute Parameters of Components in V1197 Her

Parameters	Primary (star 1)	Secondary (star 2)
M	$0.30(\pm0.01)M_\odot$	$0.77(\pm0.02)M_\odot$
R	$0.54(\pm0.01)R_\odot$	$0.83(\pm0.01)R_\odot$
L	$0.18(\pm0.01)L_\odot$	$0.38(\pm0.01)L_\odot$

characteristics of the O'Connell effect have been reported recently. The O'Connell effect appeared on UCAC4436-062932 on a very short timescale (Zhou et al. 2016) and the O'Connell effect even changed from a negative one to a positive one or otherwise (Zhou et al. 2018; Zhou, & Soonthornthum 2019). Compared with the O'Connell effect on early-type contact binaries, the magnitude differences (Max I - Max II) of the O'Connell effect on late-type contact binaries are much smaller, usually less than 0.04 mag (Pribulla et al. 2011).

The formation and evolution of contact binaries is still an open issue. They may evolve from initially detached binary systems due to angular momentum loss (Bradstreet, & Guinan 1994; Li et al. 2007). Contact binaries are classified into A-subtype or W-subtype systems Binnendijk (1970). Li et al. (2008) thought that there was no evolutionary difference between A-and W-subtype systems, and that they might be just in different stages of thermal relaxation oscillation (TRO). However, Yildiz & Doğan (2013) claimed that the initial mass of the secondary star in a binary system is the key factor affecting its evolutionary status. Binary systems with initial masses of the secondary stars that are higher than $1.8(\pm 0.1)\,M_{\odot}$ will evolve into A-subtype contact binaries while binaries with initial masses lower than this evolve into W-subtype systems. Therefore, more and more observations and analyses of both A- and W-subtype contact binary systems are needed to understand the formation mechanism of W UMa-type contact binaries.

Acknowledgements We appreciate the valuable comments and suggestions of the anonymous referee. This research was supported by the National Natural Science Foundation of China (Grant Nos. 11703080 and 11703082) and the Yunnan Natural Science Foundation (No. 2018FB006). It was part of the research activities at the National Astronomical Research Institute of Thailand (Public Organization). This work has made use of data from the European Space Agency (ESA) mission *Gaia* (`https://www.cosmos.esa.int/gaia`), processed by the *Gaia* Data Processing and Analysis Consortium (DPAC; `https://www.cosmos.esa.int/web/gaia/dpac/consortium`). Funding for the DPAC has been provided by national institutions, in particular the institutions participating in the *Gaia* Multilateral Agreement.

References

Binnendijk, L. 1970, Vistas in Astronomy, 12, 217
Bradstreet, D. H., & Guinan, E. F. 1994, Interacting Binary Stars, 228
Cox, A. N. 2000, Allen′s Astrophysical Quantities (4th ed.; NewYork: Springer)
Diethelm, R. 2003, Information Bulletin on Variable Stars, 5438, 1
Diethelm, R. 2004, Information Bulletin on Variable Stars, 5543, 1
Diethelm, R. 2006, Information Bulletin on Variable Stars, 5713, 1
Gaia Collaboration, Prusti, T., de Bruijne, J. H. J., et al. 2016, A&A, 595, A1
Gaia Collaboration, Brown, A. G. A., Vallenari, A., et al. 2018, A&A, 616, A1
He, J.-J., Qian, S.-B., & Soonthornthum, B. 2016, AJ, 152, 120
He, J.-J., Qian, S.-B., Soonthornthum, B., et al. 2019, Research in Astronomy and Astrophysics, 19, 56
Li, K., Hu, S., Chen, X., et al. 2017, PASJ, 69, 79
Li, K., Xia, Q.-Q., Hu, S.-M., et al. 2018, PASP, 130, 074201
Li, K., Xia, Q.-Q., Michel, R., et al. 2019, MNRAS, 485, 4588
Li, L., Zhang, F., Han, Z., et al. 2007, ApJ, 662, 596
Li, L., Zhang, F., Han, Z., et al. 2008, MNRAS, 387, 97
Liao, W.-P., Qian, S.-B., & Sarotsakulchai, T. 2019, AJ, 157, 207
Locher, K. 2005, Open European Journal on Variable Stars, 3, 1
Nelson, R. H. 2009, Information Bulletin on Variable Stars, 5875, 1
Nelson, R. H. 2012, Information Bulletin on Variable Stars, 6018, 1
Nelson, R. H. 2016, Information Bulletin on Variable Stars, 6164, 1
Pojmanski, G. 1997, Acta Astronomica, 47, 467
Pribulla, T., Vaňko, M., Chochol, D., et al. 2011, Astronomische Nachrichten, 332, 607
Qian, S.-B., Wang, J.-J., Zhu, L.-Y., et al. 2014, ApJS, 212, 4
Qian, S.-B., He, J.-J., Zhang, J., et al. 2017, Research in Astronomy and Astrophysics, 17, 87
Qian, S.-B., Shi, X.-D., Zhu, L.-Y., et al. 2019, Research in Astronomy and Astrophysics, 19, 64
Street, R. A., Pollaco, D. L., Fitzsimmons, A., et al. 2003, Scientific Frontiers in Research on Extrasolar Planets, 405
Soonthornthum, B. 2018, Nature Astronomy, 2, 355
Terrell, D., & Wilson, R. E. 2005, Ap&SS, 296, 221
Tody, D. 1986, Proc. SPIE, 627, 733
Udalski, A., Szymanski, M., Kaluzny, J., et al. 1992, Acta Astronomica, 42, 253
Watson, C. L., Henden, A. A., & Price, A. 2006, Society for Astronomical Sciences Annual Symposium, 25, 47
Wilson, R. E., & Devinney, E. J. 1971, ApJ, 166, 605
Wilson, R. E. 2012, AJ, 144, 73
Xiao, Z., Shengbang, Q., Binghe, H., et al. 2016, PASJ, 68, 102
Yang, Y., Li, K., Li, Q., et al. 2016, PASP, 128, 44201
Yildiz, M., & Doğan, T. 2013, MNRAS, 430, 2029
Zhao, G., Zhao, Y.-H., Chu, Y.-Q., et al. 2012, Research in Astronomy and Astrophysics, 12, 723
Zhou, X., Qian, S.-B., Essam, A., et al. 2016, New Astronomy, 47, 3
Zhou, X., Qian, S., Boonrucksar, S., et al. 2018, PASJ, 70, 87
Zhou, X., & Soonthornthum, B. 2019, PASJ, 71, 39